ARTICLE

Cu-Co Composite Oxides Supported on Multi-walled Carbon Nanotubes for Catalytic Removal of CO in a H_2-rich Stream

Ning Liu, Yu-xian Gao, Wen-dong Wang*, Wei-xin Huang

CAS Key Laboratory of Materials for Energy Conversion and Department of Chemical Physics, University of Science and Technology of China, Hefei 230026, China

(Dated: Received on May 16, 2014; Accepted on May 29, 2014)

Multi-walled carbon nanotubes (MWCNT) supported Cu-Co composite oxides catalysts were prepared by an ultrasonication treatment-aided impregnation method. The structure properties of the catalysts were characterized by XRD, TEM, H_2-TPR, XPS and Raman spectra, indicating the strong interactions between Cu and Co mixed oxides as well as between metal oxides and MWCNT support. The catalytic performance of CO removal in a H_2-rich stream was examined. In contrast to the single Cu and Co catalyst, the unique performance was observed for Cu-Co composite catalysts, which features an unusual reaction pathway through the combination of CO preferential oxidation and CO methanation especially at high reaction temperature. The optimal catalyst with Cu/Co ratio of 1/8 can achieve the complete CO conversion in a wider temperature range of 150−250 °C under the space velocity as high as 120 L/(h·g), which demonstrates a promising catalyst for the effective CO removal in a H_2-rich stream.

Key words: Copper, Cobalt, Carbon nanotube, CO preferential oxidation, CO methanation

I. INTRODUCTION

The hydrogen production is one of the crucial technologies for the future hydrogen energy economy and the polymer electrolyte membrane fuel cell (PEMFC) is considered as one of the most promising environment-friendly fuel cell technologies owing to its high energy efficiency [1, 2]. The fuel processing of hydrocarbons as the most common hydrogen production method in commercial use, mainly consisting of the reforming and water gas shift reactions, may also produce appreciable amounts of CO. However, the remaining CO can easily poison the Pt-based anode of PEMFC and thus should be removed to a trace level. In contrast to the physical methods such as cryogenic separation, pressure swing adsorption, and selective diffusion of H_2, the developing approaches by catalytic removal of CO in a H_2-rich stream mainly involve the preferential oxidation (PROX) of CO and the selective CO methanation [2−4].

The CO preferential oxidation can achieve near complete CO removal at low temperature from room temperature to below 200 °C over a variety of catalysts, including supported noble metals (Pt, Ru and Rh), Au catalysts and metal oxides such as CuO-CeO_2 catalysts [3, 4], among which Cu-Ce mixed oxides catalysts have attracted much attention because of the low cost and high selectivity. However, PROX reaction is deactivated mainly due to the competitive H_2 oxidation and reduction of metal oxides at temperature higher than 200 °C. The selective CO methanation occurs at temperature above 200 °C in the presence of Ru or Ni catalysts [3], but the side reactions of CO_2 methanation and reverse water-gas shift (RWGS) may result in the undesirable H_2 consumption and CO production [2, 5]. Since both approaches have their challenges, it might be highly desired to combine their advantages and explore catalysts with the extended operating temperature window for complete CO removal in a H_2-rich stream.

Many efforts have been made to promote the activity of CuO-CeO_2 catalysts for CO PROX reactions by employing various preparation methods [6−12], doping or incorporating with other metals [12−17] and using different support materials [18−22], mainly aiming at improvement of mixed oxides interface and stabilization of Cu^+ species that play important roles in CO PROX reactions, among which the cobalt-containing catalysts are of particular interest. It has been recently reported that the optimized ternary CuO/Co_3O_4-CeO_2 catalyst exhibits not only the lowest temperature for CO complete oxidation but also the broadest temperature window for full CO conversion [17] and cobalt-containing catalysts are more selective towards CO_2 in CO PROX [16], but it is also suggested that introduction of Co leads to negative effects on the catalytic activity and

*Author to whom correspondence should be addressed. E-mail: wangwd@ustc.edu.cn, Tel.: +86-551-63603683, FAX: +86-551-63606735

resistance against CO_2 and H_2O [15]. Moreover, the Cu−Co composite oxides have been explored for the CO PROX reactions [23−25], however, the reported catalytic performance are hardly satisfactory.

Carbon nanotubes (CNT) have proven particularly attractive and competitive in catalytic processes owing to the combination of their distinctive morphology and electronic, adsorption, mechanical and thermal properties [26]. Recent research interest has been triggered in creating novel composites of CNT-confined or supported metal or oxide nanoparticles and exploring their beneficial effects on the catalytic properties [27, 28]. Considering the unique properties of CNT different from other catalyst supports, we have recently revealed the enhanced catalytic performance for CO PROX over Ru/CNT [29] and CuO-CeO_2/CNT catalysts, but the CNT-supported Cu-Co mixed oxides catalyst for CO PROX reaction has rarely been reported. In this work, the Cu-Co composite oxides supported on multi-walled carbon nanotubes (MWCNT) was investigated to explore the relation between their structure features and performance in catalytic removal of CO in a H_2-rich stream.

II. EXPERIMENTS

The pristine MWCNTs were obtained from Chengdu Organic Chemicals, China, which were pretreated by refluxing with diluted HNO_3 (37wt%) at 110 °C for 5 h and then washed and dried. The Cu-Co mixed oxides catalysts supported on MWCNT were prepared using an impregnation method aided by ultrasonication treatment. Certain amounts of $Cu(NO_3)_2{\cdot}3H_2O$ and $Co(NO_3)_2{\cdot}6H_2O$ were dissolved with acetone and the acid treated MWCNT were added afterward with the total metal oxide loading of 35wt%. The mixture was subjected to an ultrasonic treatment for 3 h and then continuously stirred to evaporate the solvent under ambient condition. The obtained sample was dried at 110 °C overnight and finally calcined at 250 °C for 2 h in Ar atmosphere. The catalysts are denoted by Cu-Co(r)/CNT, where r is the nominal atomic ratio of Cu to Co.

The phase compositions of the catalysts were analyzed by powder X-ray diffraction (XRD) with a Philips X'Pert Pro Super diffractometer (Cu Kα, λ=0.15406 nm). Transmission electron microscope (TEM) experiments were performed on a JEOL-2100F transmission electron microscope. X-ray photoelectron spectra (XPS) were acquired with an ESCALAB 250 spectrometer equipped with Al Kα radiation (1486.6 eV). The binding energies (BE) were referred to C1s at 284.8 eV. Surface atomic composition was estimated by calculating the integral of each peak using the sensitivity factor provided by the instrumental software. Raman spectra were obtained on a Renishaw inVia raman microscope at room temperature with an excitation wavelength of 532 nm. Temperature programmed reduction (TPR) was performed on a conventional system equipped with a thermal conductivity detector (TCD). 30 mg of sample was pretreated in Ar at 350 °C for 30 min prior to the analysis. The reduction was then carried out in a flow of 5%H_2/Ar mixture with a rate of 30 mL/min from room temperature to 600 °C at a linear heating rate of 10 °C/min.

The catalytic performance of CO removal in a H_2-rich stream was carried out in fixed bed reactor at atmospheric pressure. The catalyst (50 mg) was loaded into a vertical tubularquartz reactor (4 mm i.d.) and kept in the isothermal center part of the reactor. The reaction temperature was controlled using a Yudian AI-708P controller from room temperature up to 250 °C. The feed gas stream was typically composed of 1%CO, 1%O_2 and 49%H_2 balanced with N_2 at a total flow rate of 100 mL/min regulated with a set of mass flow controllers (Sevenstar D07-12A/ZM). The weight hourly space velocity (WHSV) of total gaseous reactant was as high as 120 L/(h·g). The reactants and products were analyzed by the gas chromatographs (Shimadzu GC-14C and Fuli 9750) equipped with TCD and two packed columns (molecular sieve 5A and carbon molecular sieve) for the separation of CO, O_2, H_2, CH_4 and CO_2 respectively. Concentrations of the monitored gas components were calculated on the basis of the calibration of standard gas mixture in the known quantities. The conversion (X) of CO, the selectivity (S) of O_2 towards CO_2, and the yield (Y) of CO towards CO_2 and CH_4 were calculated as follows:

$$X_{\mathrm{CO}} = \frac{[\mathrm{CO}]_{\mathrm{in}} - [\mathrm{CO}]_{\mathrm{out}}}{[\mathrm{CO}]_{\mathrm{in}}} \times 100\% \tag{1}$$

$$S^{\mathrm{O_2}}_{\mathrm{CO_2}} = \frac{0.5[\mathrm{CO_2}]}{[\mathrm{O_2}]_{\mathrm{in}} - [\mathrm{O_2}]_{\mathrm{out}}} \times 100\% \tag{2}$$

$$Y^{\mathrm{CO}}_{\mathrm{CO_2}} = \frac{[\mathrm{CO_2}]_{\mathrm{out}}}{[\mathrm{CO}]_{\mathrm{in}}} \times 100\% \tag{3}$$

$$Y^{\mathrm{CO}}_{\mathrm{CH_4}} = \frac{[\mathrm{CH_4}]_{\mathrm{out}}}{[\mathrm{CO}]_{\mathrm{in}}} \times 100\% \tag{4}$$

III. RESULTS AND DISCUSSION

The XRD patterns of Cu-Co/CNT catalysts with different Cu/Co molar ratios are indicated in Fig.1. The most intense diffraction peak of MWCNT corresponds to (002) plane reflection of graphite (JCPDC 75-1621), which is evident for all the supported catalysts. The diffraction peaks of cobalt oxides can be ascribed to the spinel phase of face-centered cubic (fcc) Co_3O_4 (JCPDS 78-1970) for Co/CNT catalyst, while those of copper oxides are indexed to bulk CuO crystallites with monoclinic tenorite phase (JCPDS 89-5899) for Cu/CNT catalyst. For the Cu-Co mixed oxides with Cu/Co ratio of 1/8, only diffraction peaks ascribed to Co_3O_4 could

DOI:10.1063/1674-0068/27/05/523-529

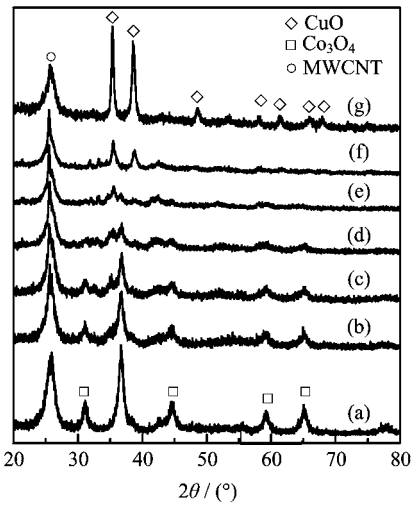

FIG. 1 XRD patterns of Cu-Co(r)/CNT catalysts. (a) Co/CNT, (b) Cu-Co(1/8)/CNT, (c) Cu-Co(2/7)/CNT, (d) Cu-Co(4/5)/CNT, (e) Cu-Co(6/3)/CNT, (f) Cu-Co(8/1)/CNT, and (g) Cu/CNT.

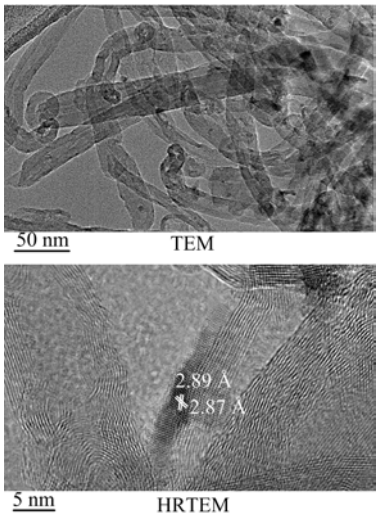

FIG. 2 TEM and HRTEM images of Cu-Co(1/8)/CNT catalyst.

be observed and almost no apparent peaks corresponding to CuO can be detected. This suggests the high dispersion of copper species or the incorpration of Cu into Co_3O_4 lattice due to the similar ionic diameter of Cu^{2+} and Co^{2+} [23, 25]. With increasing Cu/Co ratios, the peak intensity of Co_3O_4 declines while that of CuO becomes apparent. As the Cu/Co ratio increases to 8/1, only CuO could be observed implying the high dispersion of cobalt species or the incorpration of Co into CuO lattice. The crystal particle sizes of Co_3O_4 and CuO estimated by peak broadening with Scherrer's equation are listed in Table I. With an increase in the Cu/Co ratio, the crystal particle sizes of Co_3O_4 change in the range of 7.3−9.3 nm while those of CuO increase from 14.0 nm to 18.8 nm when the correspoding bulk phases are visible. The sizes of oxides supported on MWCNT are smaller than those unsupported as previously reported [23], which suggests that the MWCNT support can effectively promote the high dispersion of Cu and Co oxides. It should be mentioned that an undefined strong diffraction peak at 2θ around 25.5° appears when Cu and Co coexist on MWCNT support, however it fails to be indexed to any possible phases of alloies, mixed oxides or carbonates containing Cu and/or Co.

The dispersions of Co and Cu oxides on MWCNT were directly witnessed by TEM and HRTEM. The images of Cu-Co(1/8)/CNT catalyst are representatively shown in Fig.2. The TEM image indicates that the outer diameters of MWCNT with the supported metal oxides are mainly in the range of 25−35 nm and the metal oxides are overall supported on the outside of MWCNT with fairly homogeneous dispersion. The detailed dispersion of metal oxides on MWCNT support is observed from the HRTEM image, where only cobalt oxides are identified by a lattice spacing ca. 2.87 Å indexed to (220) planes of the cubic Co_3O_4 without any evident domains of copper oxides, in agreement with the absence of diffraction peaks of copper oxides according to XRD patterns.

TABLE I Structure characteristics for Cu-Co/CNT catalysts. The particle sizes d are in unit of nm.

Catalyst	Cu/Co[a]	Cu/Co[b]	d_{CuO}	$d_{Co_3O_4}$	I_D/I_G
Co/CNT				8.8	0.88
Cu-Co(1/8)/CNT	0.13	0.09		9.1	0.89
Cu-Co(2/7)/CNT	0.29	0.10		9.3	0.92
Cu-Co(4/5)/CNT	0.80	0.30		7.3	0.84
Cu-Co(6/3)/CNT	2.00	0.69	14.0	7.7	0.87
Cu-Co(8/1)/CNT	8.00	2.40	14.3		0.96
Cu/CNT			18.8		0.91

[a] Cu/Co ratio according to the nominal composition.
[b] Cu/Co ratio determined by XPS.

Raman spectra of the various catalysts are compared in Fig.3, which indicates two strong characteristic vibration modes for all samples, one D-band around 1344 cm^{-1} originated from the disordered structures in carbon materials and the other G-band at about 1577 cm^{-1} caused by the graphite carbon with high degree of symmetry or order [29, 30]. The integrated intensity ratio of the peaks (I_D/I_G) can be used to compare the relative degree of defects in CNT as listed in Table I. The Cu-Co/CNT catalysts exhibit much less I_D/I_G ratio around 0.84−0.96 than that of the pretreated MWCNT support only at 1.10, which suggests that the highly dispersed Cu and Co oxides prefer anchoring on the defect structure sites of CNT. It also implies that there might be a strong interaction between the oxides particles and MWCNT support, consistent with previous studies on metal or metal oxides prefer-

DOI:10.1063/1674-0068/27/05/523-529

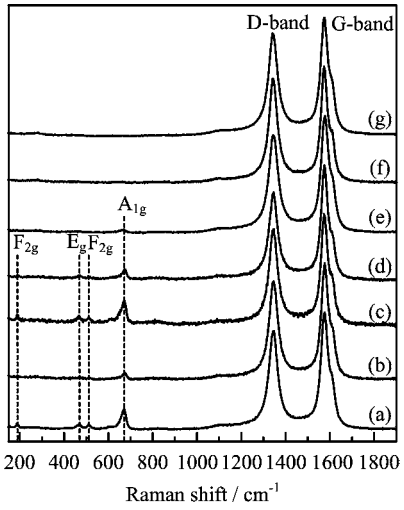

FIG. 3 Raman spectra of Cu-Co(r)/CNT catalysts. (a) Co/CNT, (b) Cu-Co(1/8)/CNT, (c) Cu-Co(2/7)/CNT, (d) Cu-Co(4/5)/CNT, (e) Cu-Co(6/3)/CNT, (f) Cu-Co(8/1)/CNT, and (g) Cu/CNT.

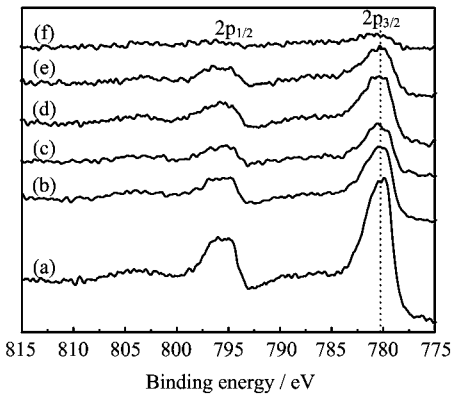

FIG. 4 Co2p core level spectra of Cu-Co(r)/CNT catalysts: (a) Co/CNT, (b) Cu-Co(1/8)/CNT, (c) Cu-Co(2/7)/CNT, (d) Cu-Co(4/5)/CNT, (e) Cu-Co(6/3)/CNT, and (f) Cu-Co(8/1)/CNT.

entially trapped by the defects or attached to the functional groups on CNT surface [31, 32]. Meanwhile, four Raman peaks of Co_3O_4 are visible for Co/CNT catalyst at 188 cm^{-1} (F_{2g}), 468 cm^{-1} (E_g), 510 cm^{-1} (F_{2g}), and 671 cm^{-1} (A_{1g}) [33, 34]. Some of these peaks are also observed for Cu-Co/CNT catalysts with the increasing Cu/Co ratio up to 4/5 in line with the XRD result; however, no peak of CuO is observable probably owing to the strong absorption effect of MWCNT support.

The surface composition and chemical states of Co and Cu were examined by XPS analysis. The surface Cu/Co ratio determined by XPS is much less than the bulk Cu/Co ratio according to the nominal composition (Table I), similar to the previous result of the unsupported Co-Cu mixed oxides [35], which may also be ascribed to the different interaction between

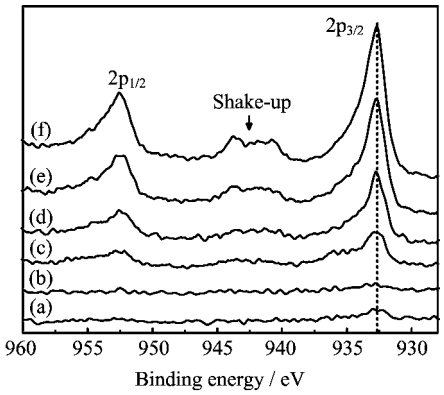

FIG. 5 Cu2p core level spectra of Cu-Co(r)/CNT catalysts. (a) Cu-Co(1/8)/CNT, (b) Cu-Co(2/7)/CNT, (c) Cu-Co(4/5)/CNT, (d) Cu-Co(6/3)/CNT, (e) Cu-Co(8/1)/CNT, and (f) Cu/CNT.

metal oxides and MWCNT support. Figure 4 shows the Co2p core level spectra of Cu-Co/CNT catalysts. All the Co-containing catalysts exhibit the $2p_{3/2}$ main peak with the binding energy centered in the range of 779.8−780.4 eV and a satellite peak at higher BE, which is close to that for Co_3O_4 and points to a simultaneous presence of Co^{2+} and Co^{3+} species [23, 35]. Figure 5 shows the Cu2p core level spectra of Cu-Co/CNT catalysts. For bulk copper oxides, the binding energy of $2p_{3/2}$ peak is centered at 932.5 eV for Cu^+ of Cu_2O, in contrast to 933.8 eV for Cu^{2+} of CuO with broad shake-up peaks around 940−945 eV [36]. As for the Cu-Co/CNT catalysts with Cu/Co ratios above 4/5, the $2p_{3/2}$ peak with BE centered at 932.7−932.9 eV and broad shake-up peaks indicate the major presence of CuO, while the relative intensity of the shake-up to main $2p_{3/2}$ peak less than 0.55 suggests the existence of partially reduced copper species [37]. However, quantitative analysis of Cu oxidation states could not be established not only because of the unfavorable Cu2p signal of the Cu-Co/CNT catalysts with Cu/Co ratios below 2/7, but also the possible self-reduction of highly dispersed Cu species as a result of exposure to the X-rays in the high-vacuum environment of XPS instrument [21].

Figure 6 compares the normalized H_2-TPR profiles to depict the reducibility of Cu-Co/CNT catalysts. In accordance with the XRD result of bulk Co_3O_4 phase for Co/CNT catalyst, the peaks centered at 302 and 445 °C correspond to the two-step reduction from Co_3O_4 to CoO and then metallic cobalt [23, 25]. In addition, a small peak centered around 200 °C may be due to the reduction of highly dispersed Co species in the form of CoO(OH) to Co_3O_4 [38]. The reduction of Cu-Co composite oxides can occur at temperatures apparently lower than those for Co_3O_4. When Cu/Co ratios increase from 1/8 to 2/7, the TPR profiles of composite oxides with low Cu content mainly feature two reduction peaks similar to Co_3O_4, but the much lower tem-

DOI:10.1063/1674-0068/27/05/523-529

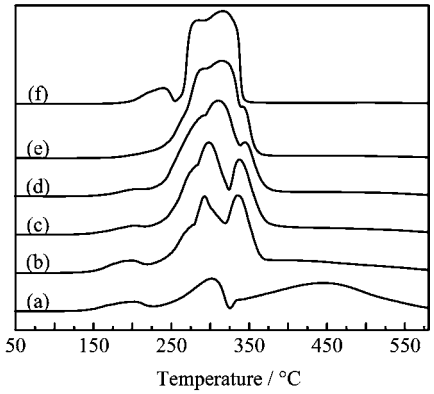

FIG. 6 H_2-TPR profiles of Cu-Co(r)/CNT catalysts. (a) Co/CNT, (b) Cu-Co(1/8)/CNT, (c) Cu-Co(2/7)/CNT, (d) Cu-Co(4/5)/CNT, (e) Cu-Co(6/3)/CNT, and (f) Cu-Co(8/1)/CNT.

perature around 295 and 336 °C, respectively. With increasing Cu/Co ratios, the TPR profile gradually resembles that of single-step reduction for CuO, which approximately occurs between 250 and 350 °C owing to different structures of catalysts and experimental conditions [23, 25]. The result suggests the promoted reducibility of Cu-Co composite catalysts, implying a strong interaction between copper and cobalt [23, 25, 35]. Moreover, the effect of support should be taken into consideration since the facilitated reduction of CuO due to the promoted electron transfer by CNT [32, 39], which may also modify the redox properties Cu-Co/CNT catalysts and be expected to promote the catalytic performance of CO removal in a H_2-rich stream.

The influence of Cu/Co ratios on the catalytic performances of Cu-Co/CNT catalysts is shown in Fig.7 for CO removal in H_2-rich stream on dependence of the reaction temperature. For the single oxide catalyst, Co/CNT is much more active than Cu/CNT for CO conversion (Fig.7(a)), in agreement with the previous result on the unsupported oxides catalysts for CO-PROX [23]. The Co/CNT catalyst can completely remove CO at 170 °C, while Cu/CNT only reaches CO conversion of 18.5% at 210 °C. In the case of Cu-Co composite catalysts, the introduction of small amount of Cu can effectively promote the catalytic performance. For Cu-Co(1/8)/CNT catalyst, it is remarkable to notice that the complete removal of CO can be achieved in a quite wide temperature range from 150 °C to 250 °C. When increasing Cu/Co ratio to 2/7, the activity begins to decline by the CO conversion decreasing into 97%−98% in the temperature region of 150−250 °C except only the complete CO removal at 170 °C. With the further increasing Cu/Co ratio, the activities of Cu-Co/CNT catalysts are even worse than that of Co/CNT as observed from the CO conversion descending more rapidly at higher reaction temperature. Meanwhile, the selectivity toward CO_2 (Fig.7(b)) can only attain nearly

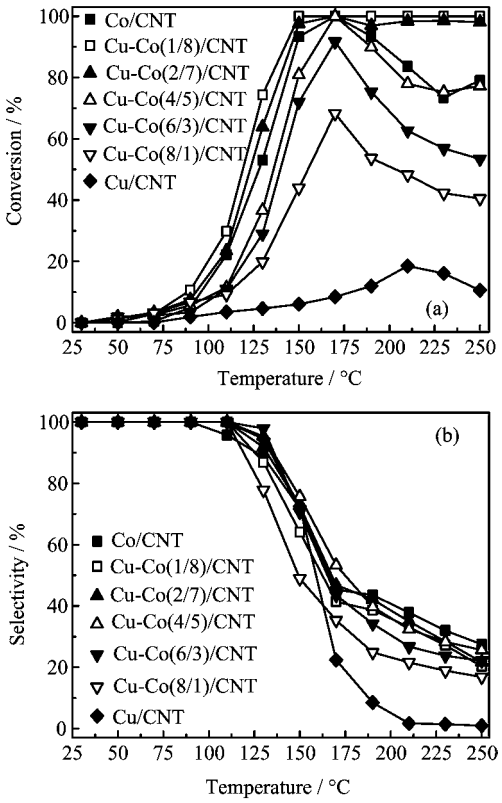

FIG. 7 Temperature dependence of (a) CO conversion and (b) CO_2 selectivity for CO removal in H_2-rich stream over Cu-Co(r)/CNT catalysts.

100% at reaction temperature lower than 130 °C when the CO conversion is far from the complete removal. It is observed that the CO_2 selectivity basically decreases with the Cu content of Cu-Co/CNT catalysts. Although Cu-Co(1/8)/CNT catalyst exhibits slightly lower CO_2 selectivity than others in some temperature region, it is practically insignificant for higher CO_2 selectivity at rather lower CO conversion with respect to the reaction of CO removal in H_2-rich stream.

The present results reveal some unusual catalytic properties of Cu-Co/CNT catalysts for the reaction of CO removal in H_2-rich stream. In comparison with the unsupported Cu-Co mixed oxides catalysts [23, 25] with the comparable Cu/Co ratio, the Cu-Co(1/8)/CNT catalyst can achieve complete CO conversion in the much wider reaction temperature range under the space velocity as high as 120 L/(h·g). Although the Cu-Ce mixed oxides system usually exhibits a greater CO_2 selectivity [6−22], the severe deactivation in CO conversion generally occurs at temperature near 200 °C due to the reduction of copper oxides, which considerably inhibits the CO-PROX performance by promoting the competitive H_2 oxidation. In contrast, the CO conversion can remain almost complete for Cu-Co/CNT catalysts with small amount of Cu, especially for Cu-Co(1/8)/CNT catalyst, despite the apparently decreased CO_2 selec-

DOI:10.1063/1674-0068/27/05/523-529

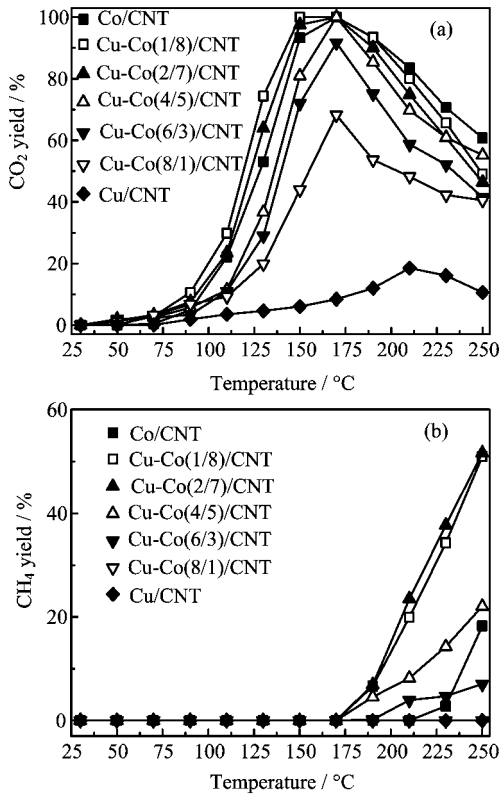

FIG. 8 Temperature dependence of the yield of CO towards (a) CO_2 and (b) CH_4 for CO removal in a H_2-rich stream over Cu-Co(r)/CNT catalysts.

tivity. Hence, there must be an additional reaction pathway rather than the preferential oxidation of CO to CO_2 accounting for the complete CO conversion at high temperature, which is examined by the yield of CO towards possible products CO_2 and CH_4 in detail.

As shown in Fig.8, the influence of Cu/Ce ratios on the yields of CO_2 and CH_4 converted from CO is compared on the reaction temperature dependence. For the temperature region below 170 °C, the CO_2 yield (Fig.8(a)) is identical with the CO conversion for all Cu-Co/CNT catalysts, accompanied by the fact that there is no CH_4 yield (Fig.8(b)). Co/CNT catalyst is much more active than Cu/CNT for conversion of CO to CO_2, while the introduction of small amount of Cu can promote the CO_2 yield for Cu-Co/CNT catalysts with Cu/Co ratios of 1/8 and 2/7. As the reaction temperature increases to above 170 °C, the CO_2 yield starts to descend for all the Co-containing catalysts due to the reduction of copper oxides to metallic Cu, which results in the performance for CO_2 yield mainly decreasing with the content of Co. At the same time, the yield of CO towards CH_4 comes into effect to various extent for different Cu-Co/CNT catalysts. In contrast to that there is no CH_4 yield for Cu/CNT catalyst in the whole temperature region, the CH_4 yield of Co/CNT catalyst is initiated at 230 °C and becomes apparent at 250 °C, because of the partial reduction of cobalt oxides and thus the formation of metallic Co that is capable of catalyzing CO methanation [40]. It is noiced that the introduction of Cu can greatly enhance the CH_4 yield of the mixed Cu-Co/CNT catalysts, in accordance with the TPR result of the promoted reducibility of Cu-Co composite catalysts. The optimzed performance in CH_4 yield observed for Cu-Co(1/8)/CNT and Cu-Co(2/7)/CNT catalysts is initiated at 190 °C and reaches more than 50% at 250 °C. The reaction pathway is mostly possible through the direct CO methanation ($CO+3H_2=CH_4+H_2O$) rather than CO_2 methanation ($CO_2+4H_2=CH_4+2H_2O$) since there is no significant reverse water-gas shift reaction ($CO_2+H_2=CO+H_2O$) over Cu and Co oxides based catalysts [25].

IV. CONCLUSION

The Cu-Co composite oxides catalysts supported on MWCNT have been prepared and examined by versatile characterization techniques. The results reveal the fine dispersion of Cu and Co oxides on MWCNT, which could induce the strong interaction between Cu and Co mixed oxides as well as between metal oxides and MWCNT support. The reducibility of Cu-Co composite catalysts is promoted due to the strong interaction between the metal oxides that may favorably attach to the defects of MWCNT support as evidence from the Raman spectra. The Cu-Co/CNT catalysts exhibit unique catalytic performance of CO removal in a H_2-rich stream, featuring the combination of CO preferential oxidation and CO methanation especially at high reaction temperature. The optimal performance is obtained for the catalyst with Cu/Co ratio of 1/8, attaining the complete CO conversion in the temperature range of 150−250 °C under the space velocity as high as 120 L/(h·g). Though the CO_2 yield from CO oxidation declines above 170 °C for Cu-Co(1/8)/CNT catalyst, the simultaneously increasing CH_4 yield from CO methanation makes compensation for achieving the complete CO conversion, which suggests Cu-Co/CNT as promising catalysts for the effective CO removal in a H_2-rich stream through a novel strategy by combining CO preferential oxidation with CO methanation.

V. ACKNOWLEDGEMENTS

This work was supported by the Anhui Provincial Natural Science Foundation (No.1408085MB25).

[1] X. Z. Yuan, H. Li, S. S. Zhang, J. Martink, and H. J. Wang, J. Power Sources **196**, 9107 (2011).
[2] J. D. Holladay, J. Hu, D. L. King, and Y. Wang, Catal. Today **139**, 244 (2009).

DOI:10.1063/1674-0068/27/05/523-529

[3] E. D. Park, D. Lee, and H. C. Lee, Catal. Today **139**, 280 (2009).
[4] N. Bion, F. Epron, M. Moreno, F. Mariño, and D. Duprez, Topics Catal. **51**, 76 (2008).
[5] P. Panagiotopoulou, D. I. Kondarides, and X. E. Verykios, Appl. Catal. A **344**, 45 (2008).
[6] G. Avgouropoulos and T. Ioannides, Appl. Catal. B **67**, 1 (2006).
[7] R. Kydd, W. Y. Teoh, K. Wong, Y. Wang, J. Scott, Q. H. Zeng, A. B. Yu, J. Zou, and R. Amal, Adv. Funct. Mater. **19**, 369 (2009).
[8] D. Gamarra, C. Belver, M. Fernandez-Garcia, and A. Martinez-Arias, J. Am. Chem. Soc. **129**, 12064 (2007).
[9] H. Yen, Y. Seo, S. Kaliaguine, and F. Kleitz, Angew. Chem. Int. Ed. **51**, 12032 (2012).
[10] M. Meng, Y. Q. Liu, Z. S. Sun, L. J. Zhang, and X. T. Wang, Int. J. Hydrog. Energy **37**, 14133 (2012).
[11] A. P. Jia, G. S. Hu, L. Meng, Y. L. Xie, J. Q. Lu, and M. F. Luo, J. Catal. **289**, 199 (2012).
[12] E. Moretti, M. Lenarda, P. Riello, L. Storaro, A. Talon, R. Frattini, A. Reyes-Carmona, A. Jimenez-Lopez, and E. Rodriguez-Castellon, Appl. Catal. B **129**, 556 (2013).
[13] J. W. Park, J. H. Jeong, W. L. Yoon, H. Jung, H. T. Lee, D. K. Lee, Y. K. Park, and Y. W. Rhee, Appl. Catal. A **274**, 25 (2004).
[14] Z. W. Wu, H. Q. Zhu, Z. F. Qin, H. Wang, L. C. Huang, and J. G. Wang, Appl. Catal. B **98**, 204 (2010).
[15] J. Li, Y. X. Han, Y. H. Zhu, and R. X. Zhou, Appl. Catal. B **108**, 72 (2011).
[16] J. L. Ayastuy, E. Fernandez-Puertas, M. P. Gonzalez-Marcos, and M. A. Gutierrez-Ortiz, Int. J. Hydrog. Energy **37**, 7385 (2012).
[17] Y. N. Chen, D. S. Liu, L. J. Yang, M. Meng, J. Zhang, L. R. Zheng, S. Q. Chu, and T. D. Hu, Chem. Eng. J. **234**, 88 (2013).
[18] V. Ramaswamy, S. Malwadkar, and S. Chilukuri, Appl. Catal. B **84**, 21 (2008).
[19] V. P. Pakharukova, E. M. Moroz, V. V. Kriventsov, D. A. Zyuzin, G. R. Kosmambetova, and P. E. Strizhak, Appl. Catal. A **365**, 159 (2009).
[20] C. L. Gu, S. H. Lu, J. Miao, Y. A. Liu, and Y. Q. Wang, Int. J. Hydrog. Energy **35**, 6113 (2010).
[21] X. B. Li, X. Y. Quek, D. Ligthart, M. L. Guo, Y. Zhang, C. Li, Q. H. Yang, and E. J. M. Hensen, Appl. Catal. B **123**, 424 (2012).
[22] C. J. Tang, J. F. Sun, X. J. Yao, Y. Cao, L. C. Liu, C. Y. Ge, F. Gao, and L. Dong, Appl. Catal. B **146**, 201 (2014).
[23] D. B. Li, X. H. Liu, Q. H. Zhang, Y. Wang, and H. L. Wan, Catal. Lett. **127**, 377 (2009).
[24] M. P. Woods, P. Gawade, B. Tan, and U. S. Ozkan, Appl. Catal. B **97**, 28 (2010).
[25] S. Varghese, M. G. Cutrufello, E. Rombi, C. Cannas, R. Monaci, and I. Ferino, Appl. Catal. A **443/444**, 161 (2012).
[26] P. Serp, M. Corrias, and P. Kalck, Appl. Catal. A **253**, 337 (2003).
[27] P. Serp and E. Castillejos, ChemCatChem **2**, 41 (2010).
[28] X. L. Pan and X. H. Bao, Accounts Chem. Res. **44**, 553 (2011).
[29] Y. X. Gao, K. M. Xie, S. Y. Mi, N. Liu, W. D. Wang, and W. X. Huang, Int. J. Hydrog. Energy **38**, 16665 (2013).
[30] Y. R. Shin, I. Y. Jeon, and J. B. Baek, Carbon **50**, 1465 (2012).
[31] Y. M. Dai, T. C. Pan, W. J. Liu, and J. M. Jehng, Appl. Catal. B **103**, 221 (2011).
[32] S. Q. Song and S. J. Jiang, Appl. Catal. B **117**, 346 (2012).
[33] C. W. Na, H. S. Woo, H. J. Kim, U. Jeong, J. H. Chung, and J. H. Lee, Crystengcomm **14**, 3737 (2012).
[34] M. Rashad, M. Rusing, G. Berth, K. Lischka, and A. Pawlis, J. Nanomater. ID 714853, (2013). http://dx.doi.org/10.1155/2013/714853
[35] G. Fierro, M. Lo Jacono, M. Inversi, R. Dragone, and P. Porta, Topics Catal. **10**, 39 (2000).
[36] A. Martinez-Arias, M. Fernandez-Garcia, J. Soria, and J. C. Conesa, J. Catal. **182**, 367 (1999).
[37] G. Avgouropoulos and T. Ioannides, Appl. Catal. A **244**, 155 (2003).
[38] C. W. Tang, C. B. Wang, and S. H. Chien, Thermochim. Acta **473**, 68 (2008).
[39] D. Wang, G. H. Yang, Q. X. Ma, M. B. Wu, Y. S. Tan, Y. Yoneyama, and N. Tsubaki, ACS Catal. **2**, 1958 (2012).
[40] Y. Yu, G. Q. Jin, Y. Y. Wang, and X. Y. Guo, Catal. Commun. **31**, 5 (2013).

DOI:10.1063/1674-0068/27/05/523-529